Double drive modes unimorph deformable mirror for femtosecond laser beam wavefront correction

Ying Liu, Junjie Chen, Jianqiang Ma, Baoqing Li, Jiaru Chu

Ying Liu, Junjie Chen, Jianqiang Ma, Baoqing Li, Jiaru Chu, "Double drive modes unimorph deformable mirror for femtosecond laser beam wavefront correction," Proc. SPIE 9283, 7th International Symposium on Advanced Optical Manufacturing and Testing Technologies: Design, Manufacturing, and Testing of Micro- and Nano-Optical Devices and Systems, 928311 (21 August 2014); doi: 10.1117/12.2070595

SPIE.

Event: 7th International Symposium on Advanced Optical Manufacturing and Testing Technologies (AOMATT 2014), 2014, Harbin, China

Double drive modes unimorph deformable mirror for femtosecond laser beam wavefront correction

Ying Liu[1], Junjie Chen[1], Jianqiang Ma[2], Baoqing Li[1*], Jiaru Chu[1]
[1]Department of Precision Machinery and Precision Instrumentation, University of Science and Technology of China, Hefei, China
[2]Faculty of Mechanical Engineering & Mechanics, Ningbo University, Ningbo, China
*Corresponding author: bqli@ustc.edu.cn

Abstract: Once a laser beam suffers from wavefront aberrations, the intensity of the focal spot degrades and the shape of the focus spot distorts. The same problem also exists in femtosecond laser fabrication system. The aberrations in the femtosecond laser fabrication system contain two main components: system aberrations and aberrations from the refractive index mismatch problem. Recently, adaptive optics (AO) has been used for laser beam aberrations correction to improve the light beam quality. In this paper, we introduce an adaptive optics system with double drive modes unimorph deformable mirror (DM) into the femtosecond laser fabrication system. In the experiments, the hill-climbing algorithm based on Zernike modes is used to control the DM to correct the aberrations in the close-loop manner. After correction for system aberrations and the refractive index mismatch aberrations, the shape and maximum intensity of the focal laser spot is much improved.

Keywords: adaptive optics; deformable mirror; femtosecond laser; wavefront correction

1. Introduction

Femtosecond laser technology is a kind of maskless high-precision fabrication technology. For its pulse width is very narrow, which is in the femtosecond (femtosecond=10^{-15}s) level, femtosecond laser fabrication can achieve high instantaneous power when the single pulse energy is very low and little heat effect is produced in the fabrication process. After years of development, femtosecond laser technology has been widely used in micro-nano processing field[1,2].

As it is known, once a laser beam suffers from wavefront aberrations, the intensity of the focal spot degrades and the shape of the focus spot distorts. The focal spot in the femtosecond laser fabrication system also suffers from this problem. The aberrations in the femtosecond laser fabrication system contain two main components: system aberrations and aberrations from the refractive index mismatch problem[3]. The system aberrations are from the imperfect surface quality of the optical element in the system, which are usually changeless in fabrication process. The other kind of aberrations are from the refractive index mismatch problem between the sample and the environment.

Recently, adaptive optics (AO) has been used for laser beam aberrations correction to improve the light beam quality[4,5]. In this paper, a mathematical model for the aberrations is established to analyze to effect from the refractive index mismatch aberrations. Then we introduce an adaptive optics system with double drive modes unimorph deformable mirror (DM) into the femtosecond laser fabrication system. The system aberrations and aberrations from the refractive index mismatch problem are respectively corrected in experiments. After correction for the two kinds of aberrations, the shape and maximum intensity of the focal laser spot is much improved.

7th International Symposium on Advanced Optical Manufacturing and Testing Technologies: Design, Manufacturing, and Testing of Micro- and Nano-Optical Devices and Systems, edited by Tianchun Ye, A. G. Poleshchuk, Song Hu, Proc. of SPIE Vol. 9283, 928311 · © 2014 SPIE · CCC code: 0277-786X/14/$18 · doi: 10.1117/12.2070595

2. **Mathematical model for refractive index mismatch aberrations**

The mathematical model for the refractive index mismatch aberrations is built here based on the scalar diffraction theory. The objective lens is assumed to be immersed in the material with a refractive index n_1, and the refractive index of sample is assumed to be n_2. We select the processing point as the coordinate system's origin, so the coordinate of the interface is z=-d. Here, d is processing depth. The schematic diagram is shown in Fig.1. From the scalar diffraction theory, it is known that the optical field distribution of an arbitrarily point P_2 after the refractive interface can be calculated from the integral of all the infinitesimal in the wavefront. The three components of optical field distribution in the point P_2 can be calculated as [6]:

$$\begin{cases} I_0^e = \int_0^\alpha P(\theta_1)\sin\theta_1(t_s + t_p\cos\theta_2)\exp[-ik_0\Phi(\theta_1)]J_0(k_1r_2\sin\theta_1)\exp(-ik_2z_2\cos\theta_2)d\theta_1 \\ I_1^e = \int_0^\alpha P(\theta_1)\sin\theta_1 t_p\sin\theta_2\exp[-ik_0\Phi(\theta_1)]J_1(k_1r_2\sin\theta_1)\exp(-ik_2z_2\cos\theta_2)d\theta_1 \\ I_2^e = \int_0^\alpha P(\theta_1)\sin\theta_1(t_s - t_p\cos\theta_2)\exp[-ik_0\Phi(\theta_1)]J_2(k_1r_2\sin\theta_1)\exp(-ik_2z_2\cos\theta_2)d\theta_1 \end{cases} \quad (1)$$

Where $P(\theta_1)$ is pupil function, θ_1 and θ_2 are incidence angle and refraction angle, respectively. The t_s and t_p are Fresnel transfer coefficient, which express the radial and tangential amplitude change before and after refraction. $\Phi(\theta_1)$ is the aberration function from refractive index mismatch aberrations, which can be expressed as:

$$\Phi(\theta_1) = -d(n_1\cos\theta_1 - n_2\cos\theta_2) \quad (2)$$

By comparison of the above three integral expression, it can be found that I_1^e and I_2^e are much smaller than I_0^e, so the intensity distribution function can be calculated as:

$$I(r,z_2) = \left|\int_0^\alpha P(\theta_1)\sin\theta_1(t_s + t_p\cos\theta_2)\exp[-ik_0\Phi(\theta_1)]J_0(k_1r_2\sin\theta_1)\exp(-ik_2z_2\cos\theta_2)d\theta_1\right|^2 \quad (3)$$

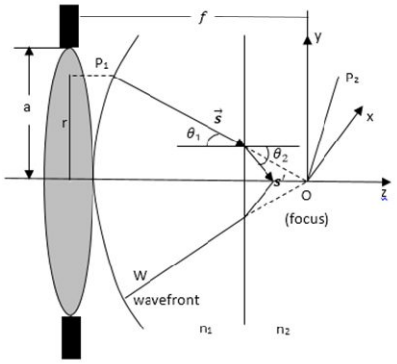

Fig. 1 The schematic diagram of the objective lens-focused spot passing the refractive index mismatch interface.

According to the established intensity distribution function, we analyze the impact of refractive index mismatch aberrations with different processing depth by the calculation. In the calculations, the center wavelength of the femtosecond laser is 800 nm, the numerical aperture (NA) of the objective lens is 0.85. The process is in the air environment, so the refractive index n_1 is 1. The refractive index of the sample is 1.458. The normalized intensity

distribution of the focal spot with different processing depth is calculated and shown in Fig. 2. From the intensity distribution in Fig.2, it can be found that the peak intensity decreases constantly with the increase of processing depth, and when the processing depth reaches 30 um, the peak intensity is only about 30% of that when the process is on the surface, and when the processing depth reaches 60 um, the difference between the main peak intensity and sub-peak intensity is not obvious, which causes multiple focal spots appear and reduces the axial processing resolution seriously.

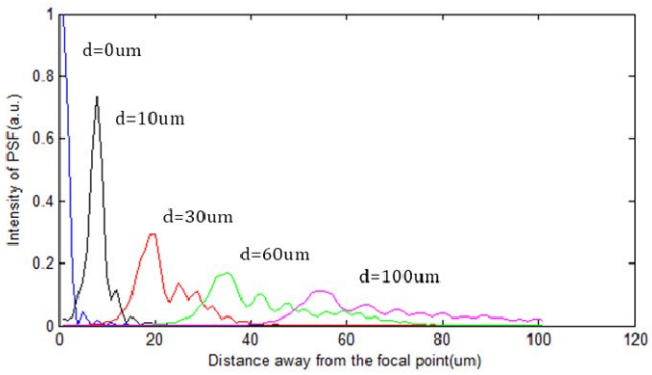

Fig.2 The intensity distribution of the focal spot with different processing depth.

3. **Experimental setup**

To correct aberrations in the femtosecond fabrication system, the adaptive optics system is introduced into the original fabrication system. In the fabrication system, the laser source is a mode-locked Ti:sapphire ultrafast oscillator(Coherent, Chamleon Vision-S) with central wavelength at 800 nm, pulse duration of 75 fs, and repetition rate at 80 MHz. The average power is about 3W, modulated by a power attenuator consisted of a half wave plate and a Glan laser prism. After passing a beam expander, the beam aperture is about 10mm, which is matched with the effective aperture of the deformable mirror. In fabrications, photoresist SZ-2080(provided by IESL-FORTH , Greece) is used as sample to be fabricated and the objective lens used here is 50X, which has a numerical aperture equal to be 0.8. The adaptive optics system uses a home-made double drive mode unimorph piezoelectric deformable mirror[7] as the wavefront corrector, the key parameters of this deformable is as shown in Tab. 1. The adaptive optics system evaluates the aberrations in the system from the CCD camera-measured intensity distribution, and controls the deformable mirror to correct aberration using the hill-climbing algorithm based on Zernike modes[8]. The schematic of the adaptive optics integrated femtosecond laser fabrication system is shown in Fig. 3.

Tab. 1 The key parameters of the deformable mirror.

Aperture	10mm
Channels	19
Electrode pattern	Hexagon
Reflective coating	Au
Stroke	2.4μm /100V
Flatness after correction	<15nm

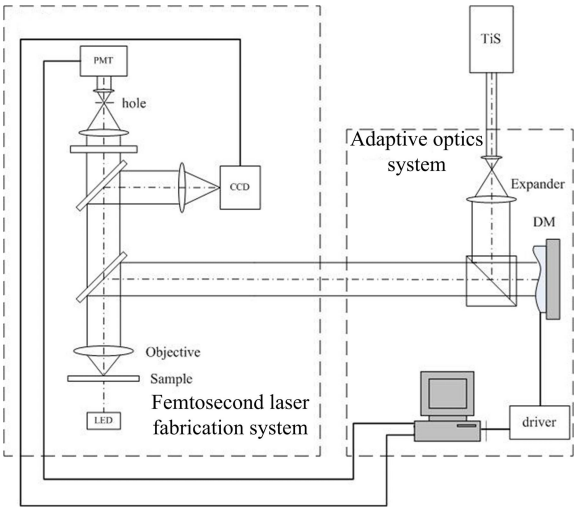

Fig. 3 The schematic of the adaptive optics integrated femtosecond laser fabrication system.

4. **Results and discussion**

In the correction process, both system aberrations and aberrations from the refractive index mismatch problem and corrected. For the system aberrations usually changeless in fabrication process, and the refractive index mismatch aberrations change with the process sample and depth change, these two kinds of aberrations are corrected separately. In correction for system aberrations, the spot is focused on the surface of the sample, and there is no aberration from refractive index mismatch problem for the spot has not entered into the sample. The CCD camera captures the reflective spot from the sample surface and measures the intensity of the spot, which is selected as the evaluate function of the control algorithm. The CCD camera-measured spot and its horizontal transverse section before and after adaptive optics correction are shown in Fig. 4. It can be found that the peak intensity is improved by about two times after correction for system aberrations. The magnified focal spot after correction is shown in Fig. 5. It can be found that circle center spot appears after correction, with the first order diffraction ring encircles it. The shape of the spot is much improved compared to that before correction.

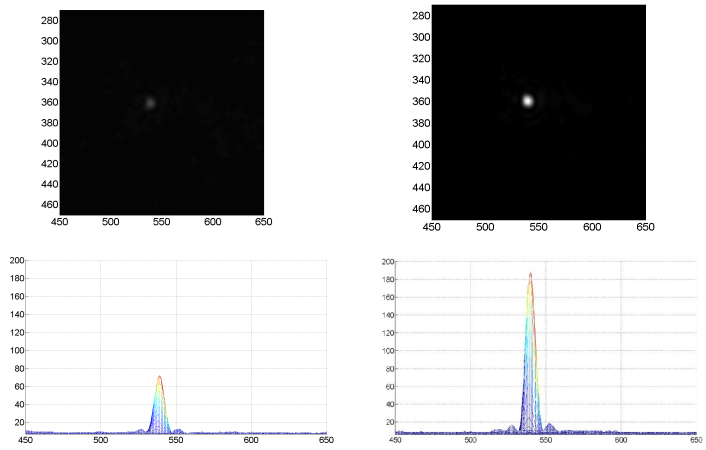

Fig. 4 The CCD camera-measured focal spot and its horizontal transverse section before and after adaptive optics correction.

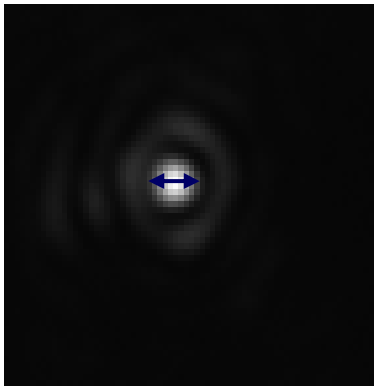

Fig. 5 The magnified focal spot after correction.

In the correction experiments of the refractive index mismatch aberrations, the control voltages for correcting system aberrations are selected as the starting point of the control algorithm. For the laser spot is focused in the sample in these experiments, there is no reflective spot from the sample. The two-photon excited fluorescence from the photoresist is selected as the evaluate function of the control algorithm. Before correction for refractive index mismatch aberrations, the impact from this kind of aberration is measured, with system aberrations completely corrected. The peak intensity of focal spot is measured in different processing depth, and the result is shown in Fig. 6. From the results, it can be found that the peak intensity decreases quickly with the processing depth increases, and the decrease curve coincides with the results from the calculation. The experiments for refractive index mismatch aberrations is carried out with the processing depth changing from 0 to 30 μm. The peak intensity curve of the focal spot before and after correction is shown in Fig. 7. It can be found that the peak intensity is improved for all the processing depth. When the processing depth increases to 10 μm, the most obvious correction effect is achieved. And as the processing depth increases further, the correction effect does not improve, which is possibly due to the saturation of the correction ability of the deformable mirror. After correction for system aberrations and the refractive index mismatch aberrations, the shape and maximum intensity of the focal laser spot is much improved.

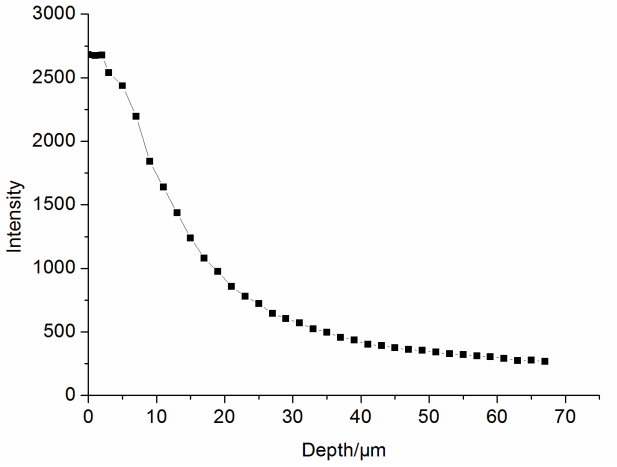

Fig. 6 The decrease of the peak intensity due to the increasement of the processing depth.

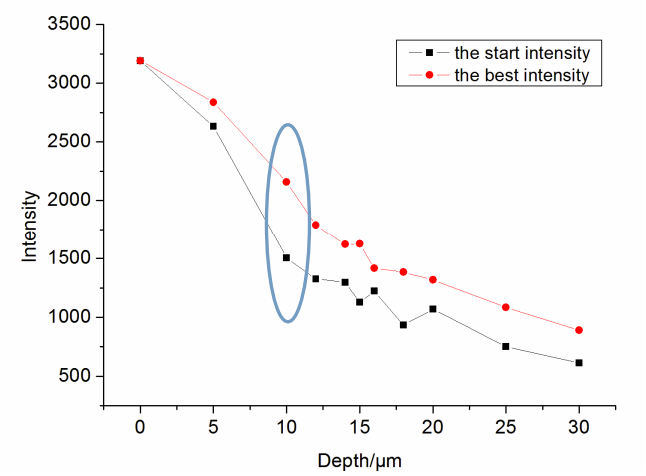

Fig. 7 The peak intensity curve of the focal spot before and after correction for refractive index mismatch aberrations.

5. Conclusion

This paper analyzes the main aberrations in the femtosecond laser fabrication system, and establishes the mathematical model for refractive index mismatch aberrations. An adaptive optics system with double drive modes unimorph deformable mirror is introduced into the femtosecond laser fabrication system. In correction experiments, system aberrations and refractive index mismatch aberrations are corrected separately. After correction for these two kinds of aberrations, the shape and maximum intensity of the focal laser spot is much improved.

Acknowledgments

This work is supported by the National Basic Research Program of China (973 Program, No. 2011CB302101), the National Natural Science Foundation of China (Grant No. 11303019) and China Postdoctoral Science Foundation (No. 2013M531521). The author also thanks the Material Science and Technology Center Development Foundation of Hefei (No.2012FXCX002), Ningbo Natural Science Foundation (2013A610047), and Project of Education Department of Zhejiang Province (Y201326728).

Reference

1. V. Sharma, E. P. Ippen, and J. G. Fujimoto, "Three-dimensional photonic devices fabricated in glass by use of a femtosecond laser oscillator," *Opt. Lett.* **30**(9), 1060-1062, (2005).

2. Hoekstra, G. Cerullo, and M. Pollnaum, "Femtosecond laser microstructuring: an enabling tool for optofluidic lab-on-chips," *Laser Photonics Rev*. **5**(3), 442-463, (2011).

3. N. Huot, E. Audouard, and R. Stoian, "Ultrafast laser writing of homogeneous longitudinal waveguides in glasses using dynamic wavefront correction," *Opt. Lett.* **16**(8), 5481-5492, (2008).

4. B.P. Cumming, A. Jesacher, M.J. Booth, T. Wilson, and M. Gu, "Adaptive aberration compensation for three-dimensional micro-fabrication of photonic crystals in lithium niobate,"*Opt. Express* **19**(10), 9419-9425, (2011).

5. S. Fourmaux, S. Payeur, A. Alexandrov, C. Serbanescu, F. Martin, T. Ozaki, A. Kudryashov, and J. C. Kieffer, "Laser beam wavefront correction for ultra high intensities with the 200 TW laser system at the Advanced Laser Light Source," *Opt. Express* **16**(16), 11987-11994, (2008).

6. P. T¨or¨ok, P. Varga, G. N´emeth, "Analytical solution of the diffraction integrals and interpretation of wave-front distortion when light is focused through a planar interface between materials of mismatched refractive indices," *J. Opt. Soc. Am. A* **12**(12), 2660-2671, (1995).
7. J.Q. Ma, Y. Liu, T. He, B.Q. Li, J.R. Chu, "Double Drive Modes Unimorph Deformable Mirror for Low-Cost Adaptive Optics," *Appl. Opt*. **50**(29), 5647-5654(2011).
8. Y. Liu, J.Q. Ma, B.Q. Li, J.R. Chu, "Hill-Climbing Algorithm Based on Zernike modes for Wavefront Sensor-less Adaptive Optics," *OPT.ENG.* ***52***(1), 016601-016605 (2013).